Multiple Missing Cell Defect Modeling for QCA Devices

Vaishali H. Dhare & Usha S. Mehta

Journal of Electronic Testing
Theory and Applications

ISSN 0923-8174
Volume 34
Number 6

J Electron Test (2018) 34:623-641
DOI 10.1007/s10836-018-5766-1

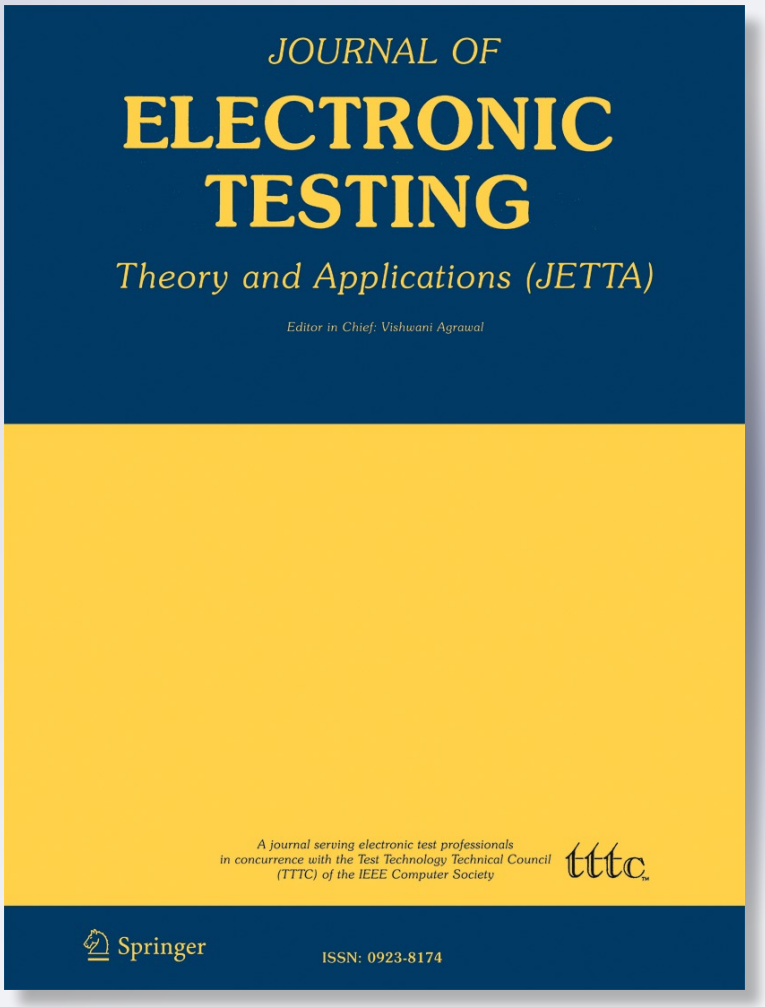

Springer

Journal of Electronic Testing (2018) 34:623–641
https://doi.org/10.1007/s10836-018-5766-1

Multiple Missing Cell Defect Modeling for QCA Devices

Vaishali H. Dhare[1] · **Usha S. Mehta**[1]

Received: 29 March 2018 / Accepted: 4 November 2018 / Published online: 20 November 2018

Abstract

Considering the limitations of CMOS technology, the Quantum-dot Cellular Automata (QCA) is emerging as one of the alternatives for Integrated Circuit (IC) Technology. A lot of work is being carried out for design, fabrication and testing of QCA circuits. In this paper, we have worked on defect analysis, fault models development and deriving various properties for QCA Majority Voter (MV) to effectively generate the test patterns for QCA circuits. It has been shown that unlike CMOS technology, single missing cell consideration is not enough for QCA technology. We have presented that the Multiple Missing Cell (MMC) defect, which is very natural at nanoscale, causes the sizable difference in functionality compared to Single Missing Cell consideration described in literature, and hence, must be considered while test generation. The proposed MMC is supported by exhaustive simulation results as well as kink energy based mathematical analysis. Further, Verilog fault models are proposed which can be used for the functional, timing verification and activation of faults caused by MMC defect. The effect of MMC on output is analyzed in stand-alone MV as well as when MV is a part of circuit. At the end, we have proposed the test properties of MV when being used as MV itself, as AND gate or OR gate. These properties may be further helpful in development of test generation algorithms.

Keywords Multiple missing cells · Majority voter · QCA · Binary wire · Fanout wire · Inverter · Kink energy

1 Introduction

In the existing CMOS technology, the scaling of the transistor is approaching its fundamental limit. Hence, substantial development in the alternative technology is required [16, 19] (http://www.itrs.net/Links/2013ITRS/Home2013.htm). These limitations steered the development of nanoscale devices like Single Electron Transistor (SET) [14], Resonant Tunneling Diode (RTD) [2] and Quantum-dot Cellular Automata (QCA) [12]. Among these, QCA has attracted more attention due to the features like low power dissipation, high device density and high switching speed. QCA is an array of cells in which each cell consists of four or six quantum dots. The basic devices in the QCA are MV, inverter, binary wire, fanout wire and L-shaped wire [25]. Each QCA synthesis circuit will consist of a network of MVs and inverters.

Due to the nanoscale of molecular QCA devices, the fabrication of QCA devices is more susceptible to defects. These defects cause unwanted functionality of the QCA devices and circuits. Fabrication of the QCA circuit involves two phases namely synthesis and deposition. In synthesis phase, the cells are manufactured and in deposition phase, these cells are deposited on the substrate [6]. The defect classification and survey of all QCA defects are presented in [3].

There are two major defects: Missing cell and cell displacement. It is notable fact that QCA devices and circuits are more susceptible to the deposition phase defects. Single missing cell deposition phase defect is discussed in the literature [17]. The single-stuck-at modeling is the most widely used in CMOS technology and multiple stuck at is overlooked many of the times considering sufficient fault coverage. Unlike CMOS, in emerging technology like QCA, the multiple missing cells cannot be ignored without necessary justification for the same. In this paper, it has been shown that the multiple missing cells have different effects on the QCA devices than the effects observed so

Responsible Editor: M. B. Tahoori

✉ Vaishali H. Dhare
vaishali.dhare@nirmauni.ac.in

Usha S. Mehta
usha.mehta@nirmauni.ac.in

[1] Institute of Technology, Nirma University, Ahmedabad, Gujarat, India

far in case of Single Missing Cell (SMC). In this paper, Multiple Missing Cells (MMC) fault models for various QCA devices is proposed and its corresponding stuck at fault sets are identified. The proposed MMC defect modeling is backed by the extensive simulation analysis. These simulation results are further supported by Kink energy based mathematical analysis. We have presented the kink energy based analytical method to decide the output cell polarization of QCA primitive, MV in case of multiple missing cells.

Further, the modules for QCA devices covering the fault set caused by the MMC defect are developed in Verilog. The effect of proposed MMC defect modeling and its faults are analysed at the circuit level for QCA EXOR gate using QCADesigner and proposed Verilog modules. At the end, test vector sets in case of fault caused by single missing and multiple missing cells are compared.

The main contribution of the paper is as follows:

1. Novel defect modeling, Multiple Missing Cell (MMC) is proposed for the QCA devices MV, inverter, binary wire, fanout wires and L-shaped wires.
2. Stuck at fault sets corresponding to MMC defect for QCA devices are identified in this work.
3. The proposed MMC defect is validated by the kink energy based analytical method.
4. HDL-Verilog models for QCA devices are developed to verify the functionality and timing information in case of MMC defect.
5. The effect of MMC on output is analyzed in stand-alone MV as well as when MV is a part of circuit.

The contents of the paper are as follows: Section 2 presents the background and literature survey of QCA defects and single missing cell. Multiple Missing Cell defect analysis is presented in Section 3. Section 4 introduces the analytical method for the estimation of output polarization of defect free MV and MV under MMC defect. Proposed Verilog modules for MMC defect is presented in Section 5. Section 6 describes the test vector set for proposed MMC defect and stuck-at properties for MV. In Section 7, test vector sets of the single missing cell and multiple missing cell defects are compared. Section 8 concludes the paper.

2 Prerequisites

2.1 Basic QCA Cell

QCA is the array of cells in which each cell contains either four or six quantum dots with two mobile electrons as shown in Fig. 1a and b. Electron tunneling out of the cell is not possible due to the potential barriers between cells. Two free electrons reside at the corners of the cells, always diagonally due to Coulombic repulsion. The cell with quantum dot's number is shown in Fig. 1a.

Electrons are located diagonally for which cell polarization is calculated. If the electrons are located as shown in Fig. 1a cell polarization P = -1 which is encoded as binary 0 (Logic 0). In the same way, considering the location of the electron as shown in Fig. 1b, the cell polarization P = +1 which is encoded as binary 1 (Logic 1). Coulombic coupling between cells causes the information flow in the QCA array [1, 9–13, 18, 20, 24].

2.2 QCA Devices

The basic QCA gates are MV and inverter, other devices are binary wire, fanout, L-shaped wire [25]. MV is a 3 inputs (A,B,C), 1 output (F), 5 cells gate. It implements the function F = M(A,B,C) = AB+BC+AC. Middle cell is device cell which has a polarization of the majority of inputs. 2-input AND (MV_AND) and OR (MV_OR) logic implementations are possible by keeping one of the inputs of MV to fixed polarization P = -1 and P = +1 respectively. The inverter as shown in Fig. 2a is another logic device of QCA.

The binary wire is shown in Fig. 2a is useful to carry the information. The binary wire is similar as interconnects of CMOS technology. Fanout wire is shown in Fig. 2a is a splitter kind of thing used to split the input into two paths.

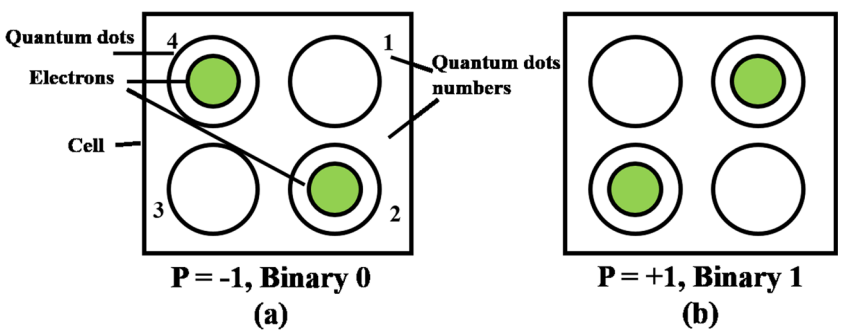

Fig. 1 QCA cell **a** with polarization P = "-1" **b** with polarization P = "+1"

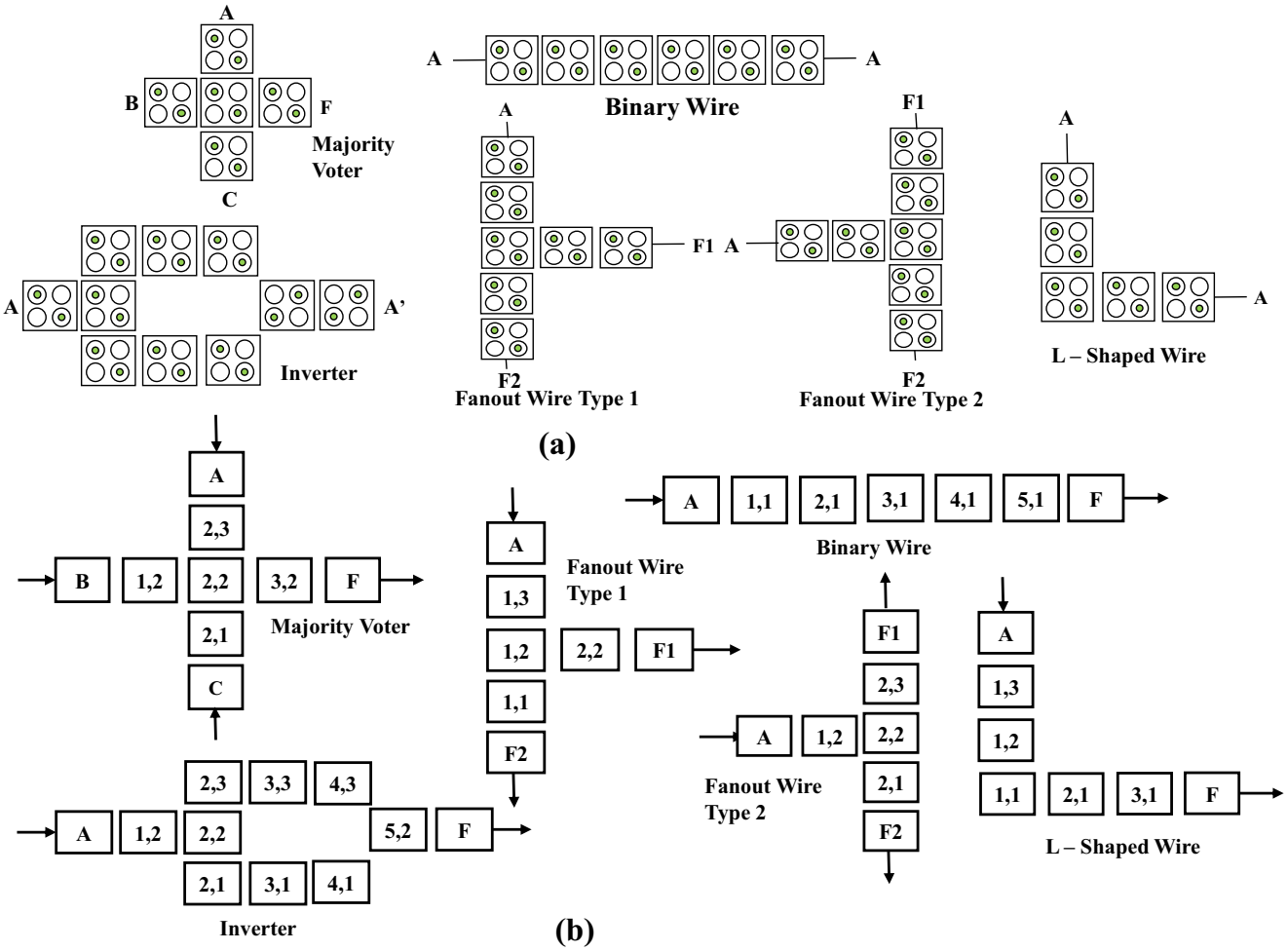

Fig. 2 **a** QCA devices **b** corresponding cell numbers

Here, two types of fanout wires, type 1 and type 2 are considered. The purpose of L-shaped wire shown in Fig. 2a is same as binary wire. Cartesian coordinates are used for the cell numbering of each device. Figure 2b shows the QCA devices with its corresponding cell numbers.

2.3 QCA Defects

QCA defects classification is shown in [3]. In molecular QCA, defects occur in synthesis and deposition phases. Defects like cell misalignment, rotation, displacement, missing and addition cell occur in the deposition phase. In misalignment defects, the cell in the QCA device may get misaligned or cell is displaced from its original direction. Rotation of cell is considered as misalignment defect.

During the lithography process, improper removal of resist causes extra cell attachment (additional) or missing cell defects. These defects also depend on the chemical compound used during the lithography. Modeling of the additional cell can be done by adding an extra cell to the periphery of device and circuit. In the same way modeling of the missing cell can be done by removing the cell from device or circuit [17].

Tahoori et al. [22, 23] described the cell misalignment and displacement defects in basic QCA primitive MV, binary wire and inverter chain.

In [8], the impact of QCA device scaling is presented. Gabriel et al. [21] analyzed the behavior of QCA building blocks under the influence of random cell displacement defect. Momenzadeh et al. [17] analyzed the single missing and additional cell defects in the QCA devices MV, inverter, fanout and L-Shaped, its corresponding stuck at fault sets are also proposed. The fault set caused by the single missing cell is mentioned in Table 1.

Dysart et al. [6] analyzed the effects of missing cell defects in QCA wire assembled by a molecular implementation.

Huang et al. [7] presented the defect characterization of sequential QCA circuits which is based on molecular QCA.

Liu et al. [15] explored the behavior of metal-dot QCA systems under stress caused by the high temperature

Table 1 Fault set caused by single missing cell [17]

Device	Fault set
MV	s-a-B
	F(A',B,C')
Inverter	s-a-A
L-shaped wire	s-a-A
Fanout	s-a-A'

operation, high speed operation, and random variation in parameter values.

Yang et al. [27] analysed the behaviour of QCA devices in presence of cell rotation. Further, they have presented a model for cell rotation effect using modified coherence vector formalism for the permissible rotational angle.

Yongqiang et al. [28] examined the effect of cell movement in horizontal and vertical directions at the same time (two-dimensions) for QCA fundamental devices MV, Inverter and binary wire. Basic fault model for single input missing cell deposition defect for QCA MV is developed in [5].

Since self-assembly fabrication process for molecular QCA is prone to defects, in near future if QCA circuit and system would exists, the key issue, defects must be addressed to avoid the failure of it. Fault analysis of QCA combinational circuit at layout and logic level is presented in [4].

3 Proposed Multiple Missing Cells Defect Modeling

3.1 Simulation Parameters

To analyze the MMC defect by simulation, two different simulation parameter sets of QCADesigner [26] as mentioned in Table 2 are considered.

Table 2 Simulation parameter

Parameter	Simulation set up 1	Simulation set up 2
Simulation engine	Bistable approximation & Coherence vector	
Cell width	18nm	10nm
Cell height	18nm	10nm
Dot diameter	5nm	2.5nm
Cell to cell distance	2nm	2nm
Radius of effect	50nm	40nm

Both the simulation engines, bistable approximation and coherence vector of QCADesigner are used. The purpose of selection of the two engines is to compare the effects of MMC defect on the QCA devices in both the engines. Also, the cell size 18nm × 18nm is selected as it is the standard size in the simulator. The dot diameter, cell to cell distance and radius of effect are selected according to cell size. Another cell size 10nm × 10nm is taken for both the simulation engines to analyze the effects of MMC defect in case of cell size variations. The QCA cell parameters are shown in Fig. 3a. Other simulation parameters like relative permittivity, clock high and low values are kept constant. The default value of relative permittivity approximately 12.9 for GaAs/AlGaAs is considered for all the simulations. However, the scaling effect of these parameters on the defect analysis are also discussed in this section.

The interaction effect of one cell on the other decays inversely with the fifth power of the distance between cells [12]. The radius of effect is a distance from the centre of one cell to another cell. All the neighboring cells coming within this radius effect would interact with this cell. As shown in Fig. 3b, only the cells within the radius of effect interact with it. Cells outside of the radius of effect do not interact with the reference cell as shown in Fig. 3b.

3.2 MMC Defect Analysis

QCA devices MV, inverter, binary wire, fanout wires and L-shaped wire with cell numbers according to the Cartesian coordinates shown in Fig. 2b are considered. External cells connected to input and output cells of each primitive are considered as defect free. The MMC defects in these devices are analyzed in the following sub sections:

3.2.1 Majority Voter

The MMC defect in MV is analyzed and its corresponding stuck at fault sets are developed in this section. The five cell MV configuration is considered as such, in which cells (2,3), (1,2) and (2,1) are the input cells and (3,2) is the output cell. The multiple cell combination is formed and removed from the layout of MV to analyze its effect on the output of it.

Double Missing Cells

1. If at a time two input cells out of the three are missing then MV always act like a binary wire in which the output is equivalent to the remaining input. Cells (2,3)&(1,2): The output is same as C i.e. Stuck-at-C

   Cells (2,3)&(2,1): The output is same as B, i.e. Stuck-at-B

   Cells (1,2)&(2,1): The output is same as A i.e. Stuck-at-A

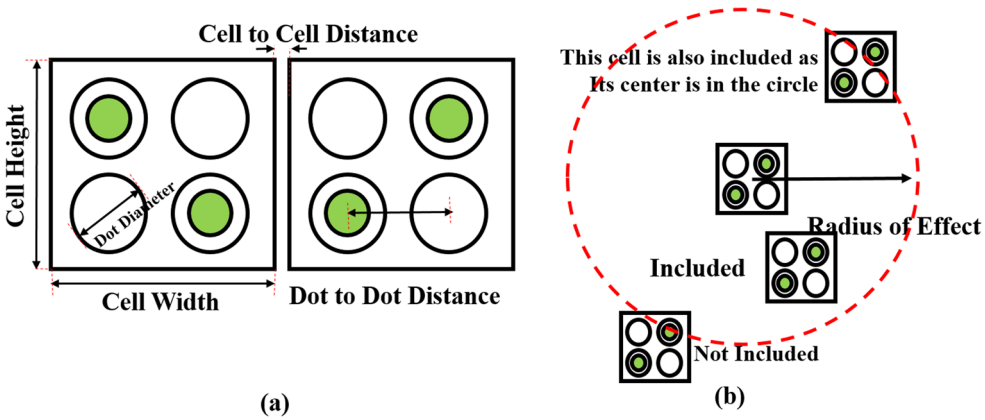

Fig. 3 Simulation parameters **a** cell parameters **b** radius of effect

The QCADesigner layout of MV with the missing cell (2,3)&(1,2) is shown in Fig. 4a and its corresponding simulation result is shown in the Fig. 4b.

2. If device cell and any one vertical input cell are missing then the output is the inversion of remaining input.

   Cells (2,3)&(2,2): The output is an inversion of remaining input, C, i.e. stuck-at-C'.

   Cells (2,1)&(2,2): The output is the inversion of remaining input A, i.e. stuck-at-A'.

3. If device cell and horizontal input cell are missing then the output of MV becomes F(A'BC').

   Cells (1,2)&(2,2): Unlike above effects, missing of the input cell (1,2) with the cell (2,2) cause the inversion of input A and C, so the output function of MV is obtained for these missing cells is F(A'BC').

4. If Output cell and any other cell out of remaining four cells, 3 inputs and 1 device cell are missing then the output of MV always observed at low polarization(LP):

   Cells (2,3)&(3,2),(1,2)&(3,2),(2,1)&(3,2) and (2,2)&(3,2): If any cell of the MV is missing with the output cell (3,2) then output at very Low Polarization (LP) is observed. It means output cell does not follow polarization either '+1' or '-1', it has very low value, approximately 0.09.

Triple Missing Cells

1. If all the three input cells are missing then the MV functionality does not alter.

   Cells (2,3)&(1,2)&(2,1): Missing of all these 3 input cells do not affect the functionality of MV since the device cell is present and all the three input cell gets interacted with this device cell because of the radius of effect.

2. If device cell and horizontal input cell are missing with the one vertical input cell then the output is an inversion of remaining vertical input cell.

   Cells (2,3)&(1,2)&(2,2): In this case, the device cell (2,2) and horizontal input cell (1,2) are missing

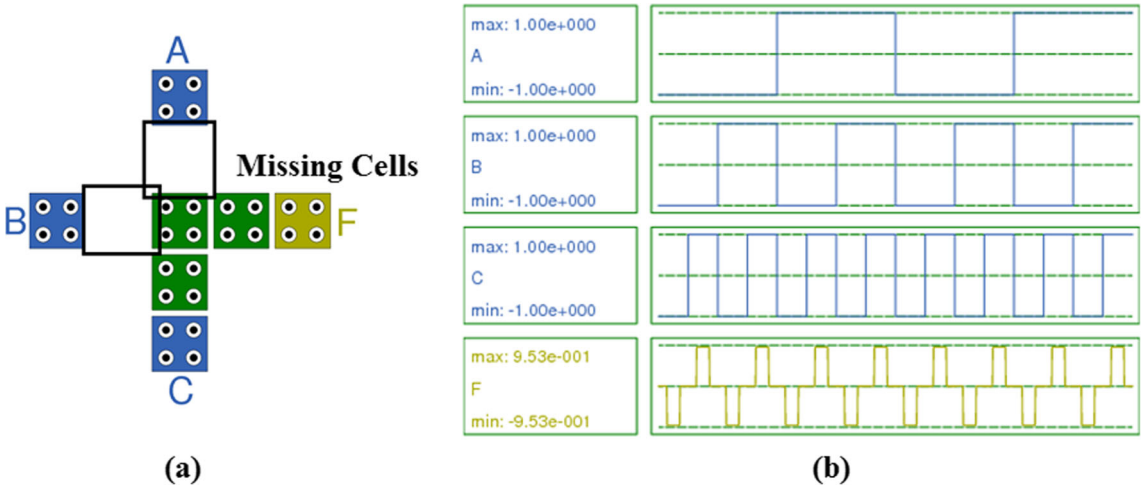

Fig. 4 MV with multiple missing cells (2,3)&(1,2) **a** layout **b** simulation result

with vertical input cell (2,3) so that the inversion of remaining vertical input cell C is observed at the output i.e. stuck-at-C'.

Cells (1,2)&(2,1)&(2,2): Similarly to the above, the output as the inversion of input A is observed i.e. stuck-at-A'.

3. If device cell and both the vertical input cells are missing then the output same as the remaining horizontal input is observed.

   Cells (2,3)&(2,1)&(2,2): Since device cell (2,2) and two vertical input cells (2,3) and (2,1) are missing, the output is same as remaining horizontal input i.e. B. Inversion of B is not observed as this cell is horizontally aligned to the output cell.
4. If output cell with any double cells are missing then the output of MV at low polarization is observed.

   Cells (2,3)&(1,2)&(3,2), (1,2)&(2,1)&(3,2), (1,2)&(2,2) &(3,2), (2,1)&(2,2)&(3,2): If Any cell pair with output cell (3,2) is missing then the low polarization at the output is observed.

Quadruple Missing Cells We have carried out the simulation extensively and observed that for missing of quadruple cells (2,3)&(1,2)&(2,1)&(2,2), the output is inversion of input C. We assume that this happens due the limitation of the simulator since missing of the quadruple cell is a hypothetical case. So, the device will no longer exist in this case and hence, output at low polarization should be considered.

Quintuple Missing Cells This is also a hypothetical case, the device will no longer exist and hence the scenario is not taken into consideration.

The MMC deposition defect analysis results of MV are summarized in Table 3.

It is observed from the above MMC defect analysis in MV that out simulated 25 combinations of multiple missing cells, the erroneous output is observed for 24 combinations i.e. MV function is not affected for only one combination. Thus, impact of MMC defect on MV in terms of number of times erroneous output obtained over total number of combinations is considered for comparison.

3.2.2 Inverter

Logically, it is very clear that for an inverter, there can be only two possible fault set i.e. the inversion is not performed i.e. the output is stuck at the input or the output is low polarization. These two faults are already covered in the single missing cell model. Anyhow, to ensure the multiple missing cell considerations, we had done the exhaustive simulation for each possibility of double, triple, quadruple, quintuple, sextuple, septuple and octuple missing cell combinations and concluded the same again with simulation results. The results are not described here as it is not of that much relevance considering the logical observations.

Table 3 MMC defect analysis results of MV

Sr. No.	Missing cell numbers	Output (F)
1	(2,3)&(1,2)	C
2	(2,3)&(2,1)	B
3	(1,2)&(2,1)	A
4	(2,2)&(2,3)	C'
5	(2,2)&(2,1)	A'
6	(2,2)&(1,2)	F(A'BC')
7	(3,2)&(2,3)	LP
8	(3,2)&(1,2)	LP
9	(3,2)&(2,1)	LP
10	(3,2)&(2,2)	LP
11	(2,3)&(1,2)&(2,1)	F(ABC)
12	(2,3)&(1,2)&(2,2)	C'
13	(1,2)&(2,1)&(2,2)	A'
14	(2,3)&(2,1)&(2,2)	B
15	(2,3)&(2,2)&(3,2)	LP
16	(2,3)&(1,2)&(3,2)	LP
17	(1,2)&(2,1)&(3,2)	LP
18	(1,2)&(2,2)&(3,2)	LP
19	(2,1)&(2,2)&(3,2)	LP
20	(2,3)&(2,1)&(3,2)	LP
21	(2,3)&(1,2)&(2,1)&(2,2)	LP
22	(2,3)&(1,2)&(2,2)&(3,2)	LP
23	(2,3)&(2,1)&(2,2)&(3,2)	LP
24	(1,2)&(2,1)&(2,2)&(3,2)	LP
25	(2,3)&(1,2)&(2,1)&(3,2)	LP

3.2.3 Binary Wire

If a single cell is missing, considering the radius of effect, the output may not be affected. But if any two or more consecutive cells are missing in the binary wire, it would affect the output depending upon the radius of effect. Further, if the output cell of binary wire is missing with the cell just before to it, then the output cannot be determined (low polarization). Low polarization effect is observed when it's output is Primary Output(PO). This is very rare case when only long binary wire is the output of a circuit that means output cell of binary wire acting as a PO of circuit.

3.2.4 Fanout Wires

Two types of fanout wire as shown in Fig. 2a, type 1 and type 2 are taken into consideration. Fanout wire of type

1 is only available in the literature [17], further, we have explored the possibility of fanout wire of type 2. The fanout wire has two outputs namely F1 and F2 so that effects of multiple missing cells on both the outputs are analyzed. In the QCA wire type namely binary wire, fanout wire and L-shaped wire, the output must be same as the input A, in the MMC defect analysis the proper obtained output in case of wires is considered as A and its inverted output as A'.

Fanout Wire Type 1 The MMC defect in fanout wire type 1 are as follows:

Double Missing Cells

1. Cells (1,3)&(1,2): In this case, output F1 gets inverted and output F2 remains same as the input.
2. Cells (1,2)&(1,1): Since cell output cell (1,1) is missing in this combination, low polarization is observed at F2 but an inversion of A is observed at the F1 since cell (1,2) is missing.
3. If any cell with the cell (2,2) is missing then low polarization is observed at output F1 and on other hand, F2 remained same as the input. Similarly, when the cell (1,1) is missing with any other cell, low polarization is observed at output F2 but F1 remained same as the input.

Triple Missing Cells For all three and four combinations of missing cells, low polarization is observed since the input cell is not interacted with the outputs F1 and F2 due to the set values of radius of effect. The MMC defect analysis for fanout wire type 1 is summarized in Table 4. Output F2 is observed as more defect tolerant.

Fanout Wire Type 2 The MMC defect in fanout wire type 2 are as follows:

Double Missing Cells

1. Cells (1,2)&(2,1): Since cell (2,1) is the output cell for F2, low polarization is observed at F2 while F1 remains as it is.
2. Cells (1,2)&(2,3): As similar to above effect, since cell (2,3) is the output cell for F1, low polarization is observed at F1 while F2 remains at it is.
3. Cells (2,1)&(2,2): F1 get inverted since cell (2,2) is missing and low polarization at F2 is observed as output cell of it, (2,1) is missing.
4. Cells (2,2)&(2,3): Similar to above effect, F2 get inverted and low polarization is observed at F1.
5. Cells (1,2)&(2,2): Missing of these cells causes the inversion at both the outputs F1 and F2.
6. Cells (2,3)&(2,1): Since cell (2,3) and (2,1) are the output cells of the F1 and F2 respectively, missing of these cells affects both the outputs. Low polarization is observed at F1 and at F2 as well.

Triple Missing Cells Due to the different structure of fanout wire type 2, missing of three cell (1,2)&(2,2)&(2,1) cause the output F1 as A' and F2 as undesired output whereas missing of cells (1,2)&(2,2)&(2,3) cause the output F2 as A' and F1 as undesired output. The MMC defect analysis for fanout wire type 2 is summarized in Table 5. Unlike the fanout wire type 1, in fanout wire type 2, both the outputs, F1 and F2 affect equally.

3.2.5 L-Shaped Wire

The MMC defect in the L-shaped wire are as follows:

Double Missing Cells

1. Only cell (1,1) is a critical cell for MMC defect in the L-shaped wire, if any other cell is missing with this cell, then the output is an inversion of the input. Otherwise,

Table 4 Multiple missing cells analysis of fanout wire type 1

Sr. No.	Missing cell numbers	Output (F1)	Output (F2)
1	(1,3)&(1,2)	A'	A
2	(1,2)&(2,2)	LP	A
3	(1,3)&(2,2)	LP	A
4	(1,3)&(1,1)	A	LP
5	(1,2)&(1,1)	A'	LP
6	(2,2)&(1,1)	LP	LP
7	(1,3)&(1,2)&(1,1)	A'	LP
8	(1,3)&(1,2)&(2,2)	LP	LP
9	(1,3)&(1,1)&(2,2)	LP	LP
10	(1,2)&(1,1)&(2,2)	LP	LP

Table 5 Multiple missing cells analysis of fanout wire type 1

Sr. No.	Missing cell numbers	Output (F1)	Output (F2)
1	(1,2)&(2,1)	A	LP
2	(1,2)&(2,3)	LP	A
3	(2,1)&(2,2)	A'	LP
4	(2,2)&(2,3)	LP	A'
5	(1,2)&(2,2)	A'	A'
6	(2,1)&(2,3)	LP	LP
7	(1.2)&(2,3)&(2,2)	LP	A'
8	(1,2)&(2,2)&(2,1)	A'	LP
9	(2,3)&(2,2)&(2,1)	LP	LP
10	(1,2)&(2,3)&(2,1)	LP	LP

MMC defect would not affect the functionality of L-shaped wire.
2. As similar to other devices, if output cell (3,1) is missing with any other cell then low polarization is observed at the L-shaped wire.

Triple Missing Cells

1. If more than two cells are missing with the cell (1,1) i.e for cells (1,1)&(1,2)&(1,3), then the inversion of the input at the output is observed.
2. If more than two cells are missing with the output cell (3,1) then the low polarization is observed.

MMC defect analysis of L-shaped wire is summarized in Table 6.

3.3 Scaling Effect of Simulation Parameters on MMC Defect

In addition to two sets of simulation parameters, we have also considered the scaling of simulation parameters like cell size, relative permittivity and radius of effect in case of MMC defect for MV as described below:

1. Cell Size: Similar to the concept of constant scaling in CMOS, for QCA also, to observe the scaling effect of cell size, all the cell parameters depicted in Fig. 3a must be proportionally scaled. The experiment is simulated for various cell size e.g. 10nm, 20nm, 30nm, 40nm and it is observed that same results are obtained in case of MMC defect for all these cell size scaling. Unlike linear relation between the cell size scaling and erroneous behavior in case of cell displacement and misalignment defects mentioned in [8], it has been seen that missing cell defect and its corresponding fault are independent of cell size.
2. Relative Permittivity: The default value of relative permittivity for GaAS/AlGaAs is considered as 12.9 in the QCADesigner simulator. It is observed that the simulator does not support to the value less than 12.9. In this case, the waveforms gets distorted. For values greater than 12.9, the polarization level (value) decreases since energy is inversely proportional to relative permittivity. The necessary equations are discussed in Section 4 in detail.

   Therefore, the scaling of relative permittivity causes change in the level of polarization on other hand MMC defect is independent of its scaling.
3. Radius of Effect: For the QCA devices, the variation in value of radius of effect can be a major concern for the cell displacement and misalignment defects. In case of missing cell defect, if minimum requirement of radius of effect is fulfilled then the single missing cell defect is not affected by any further change in the radius of effect value. Further, for multiple missing cells, the change of radius of effect may cause different effects for the positions of missing cell pair which can be address as future work. For this work, radius of effect is kept more than twice of the cell size.

Table 6 Multiple missing cells analysis of L-shaped wire

Sr. No.	Missing cell numbers	Output (F)
1	(1,3)&(1,2)	A
2	(1,3)&(1,1)	A’
3	(1,3)&(2,1)	A
4	(1,3)&(3,1)	LP
5	(1,2)&(1,1)	A’
6	(1,2)&(2,1)	A
7	(1,2)&(3,1)	LP
8	(1,1)&(2,1)	A’
9	(1,1)&(3,1)	LP
10	(2,1)&(3,1)	LP
11	(1,3)&(1,2)&(1,1)	LP
12	(1,3)&(1,2)&(2,1)	LP
13	(1,3)&(1,2)&(3,1)	LP
14	(1,3)&(1,1)&(2,1)	A’
15	(1,3)&(1,1)&(3,1)	LP
16	(1,3)&(2,1)&(3,1)	LP
17	(1,2)&(1,1)&(2,1)	LP
18	(1,2)&(1,1)&(3,1)	LP
19	(1,2)&(2,1)&(3,1)	LP
20	(1,1)&(2,1)&(3,1)	LP
21	(1,3)&(1,2)&(1,1)&(2,1)	LP
22	(1,3)&(1,2)&(1,1)&(3,1)	LP
23	(1,3)&(1,1)&(2,1)&(3,1)	LP
24	(1,2)&(1,1)&(2,1)&(3,1)	LP
25	(1,3)&(1,2)&(1,1)&(3,1)	LP

3.4 Comparison Between SMC and MMC Defects

Here, single missing cell defect and MMC defect in QCA devices are compared. This comparison is made in terms of percentage impact on the QCA devices i.e. the number of times the erroneous output obtained due to the missing cell defects over the total number of permutation combinations of missing cells. The percentage impact is calculated by Eq. 1.

$$\%impact = \frac{Totalnumberoferroneousoutput}{nCr} \tag{1}$$

nCr = Total possible combinations of multiple missing cells

$$nCr = \sum_{r=2}^{n-1} \frac{n!}{r!(n-r)!} \tag{2}$$

Table 7 Impact and fault set caused by multiple missing cells defect in QCA devices

Devices	Impact (in %) caused by		Fault set in case of	Fault set in case of
	Single missing cell defect [17]	Proposed multiple missing cells defect	Single missing cell defect [17]	Proposed MMC defect
MV	80	96	s-a-B	s-a-B
			F(A'BC')	F(A'BC')
			LP	LP
				s-a-A
				s-a-A'
				s-a-C
				s-a-C'
Inverter	33	55	s-a-A	s-a-A
			LP	LP
Binary wire	0	1	–	LP
Fanout wire Type1	F1-50	F1-90	s-a-A'	s-a-A'
			LP	LP
	F2-25	F2-70	LP	LP
Fanout wire Type2	–	F1-90	–	s-a-A'
		F2-90		LP
L-shaped Wire	20	88	s-a-A'	s-a-A'
				LP

Where n is a total number of cells of QCA primitive and r is multiple cells.

This comparison between the percentage impact in case of single missing cell defect and proposed MMC defect in QCA devices is reported in Table 7. Also, the fault sets caused by single missing cell defect and MMC defect for corresponding QCA primitive are mentioned in Table 7. This comparison is also shown graphically in Fig. 5.

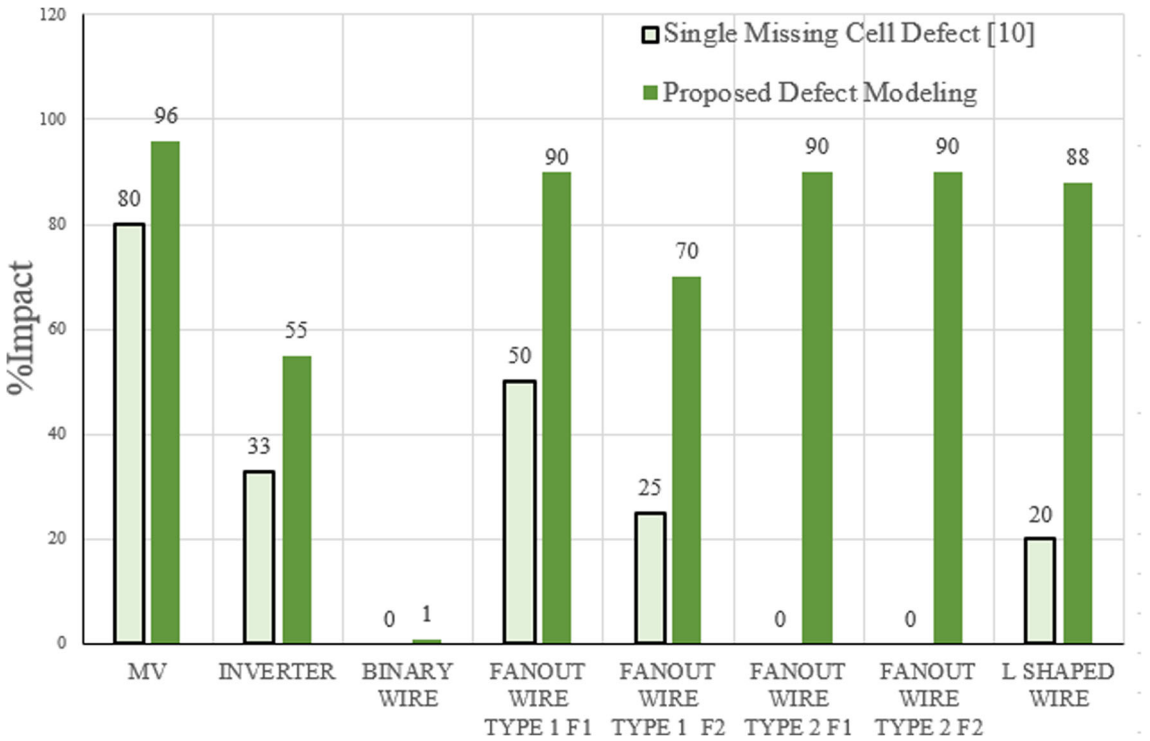

Fig. 5 Comparison between impact of single missing cells and proposed MMC defect on QCA devices

It is also observed from the number of fault sets mentioned in Table 7 for MV that, out of total 6 fault sets in case of MMC defect only 2 fault sets are covered in single missing cell defect as reported earlier in [17]. Thus, 4 faults i.e. 67% of fault sets are not covered by single missing cell defect. These uncovered faults are shown as bold entries in Table 7. Hence, in this work, we are proposing these uncovered faults for multiple missing cells in case of QCA devices like MV and others.

4 Mathematical Proof for MMC Defect

The proposed defect modeling is backed by the kink energy based mathematical analysis. For this purpose, first the kink energy is explained in detail along with the necessary equations and later the mathematical analysis for MMC is presented in length.

4.1 Kink Energy

Kink energy discussed in depth starting form the QCA cell basic equation. The polarization (P) of the cell shown in Fig. 1a and b is calculated by Eq. 3 [25].

$$P = \frac{(\rho_1 + \rho_3) - (\rho_2 + \rho_4)}{\rho_1 + \rho_2 + \rho_3 + \rho_4} \tag{3}$$

Where ρ_i is expectation value of the number operator on site (dot) for the ground state Eigen function as given by Eq. 4. Where i is the quantum dot's number 1, 2, 3, and 4 as depicted in Fig. 1a.

$$\rho_i = \langle \psi_0 | \hat{n}_i | \psi_0 \rangle \tag{4}$$

Where $|\psi_0\rangle$ is ground state of the cell and it is given in the Eq. 5.

$$|\psi_0\rangle = \sum_j \psi_j^0 |\phi_j\rangle \tag{5}$$

Where ϕ_j is the j^{th} basis vector and ψ_j^0 is the coefficient of the basis vector. It is determined by direct diagonalization of the Hamiltonian.

In two-cells i, j system, the polarization of cell j and cell i is aligned with each other. In this case, cell i is considered as a driver. In N-cell system, for single cell i, the two state model is calculated by the Hamiltonian is given in Eq. 6.

$$\hat{H}_i = \begin{pmatrix} -\frac{1}{2}\sum_j E_{i,j}^k P_j & -\gamma_i \\ \gamma_i & \frac{1}{2}\sum_j E_{i,j}^k P_j \end{pmatrix} \tag{6}$$

Where γ_i is the tunneling energy, $E_{i,j}^k$ is the kink energy between cells i and j. To understand the kink energy, first see the electrostatic energy. The electrostatic energy between two cells is used to find the state energy. The electrostatic energy between cells i and j is given by Eq. 7.

$$E^{i,j} = \frac{1}{4\pi\varepsilon_0\varepsilon_r} \sum_{n=1}^{4}\sum_{m=1}^{4} \frac{q_n^i q_m^j}{\left| r_n^i - r_m^j \right|} \tag{7}$$

Where ε_0 is the permittivity of free space, ε_r is the relative permittivity of material, q_n^i is the charge in dot n of cell i, q_m^j is the charge in dot m of cell j, r_n^j is the position of n^{th} dot in cell i, r_m^j is the position of m^{th} dot in cell j, thus $\left| n^i - r_m^j \right|$ is the distance between n^{th} dot in cell i and m^{th} dot in cell j. Thus, the Coulombic interaction between two cells can be described by the electrostatic energy. The Eq. 7 can be reduce as Eq. 8.

$$E^{i,j} = \frac{q^2}{4\pi\varepsilon_0\varepsilon_r} \sum_{n=1}^{4}\sum_{m=1}^{4} \frac{1}{\left| r_n^i - r_m^j \right|} \tag{8}$$

Equation 8 can be rewritten as Eq. 9 where D is the summations of distances between the dots in which charge is located.

$$E^{i,j} = \frac{q^2}{4\pi\varepsilon_0\varepsilon_r} \times \frac{1}{D} \tag{9}$$

All the terms of the Eq. 9 are constant except distance D. Therefore, the electrostatic energy between two cells is inversely proportional to the distance (D).

The kink energy is the difference of electrostatic energies between two cells with opposite polarization and same polarization. This concept is depicted in Fig. 6 and given in Eq. 10.

$$E_{kink}^{i,j} = E_{opposite}^{i,j} - E_{same}^{i,j} \tag{10}$$

$E_{opposite}^{i,j}$: Energy between cell i & j with opposite polarization.

$E_{same}^{i,j}$: Energy between cell i & j with same polarization.

The position of electrons i.e. polarization of the neighbouring cell from its input or adjacent cell can be found by calculating the kink energy. Kink energy is calculated using Eq. 10 which is the difference of two energies namely, $E_{opposite}$ and E_{same}. $E_{opposite}$ is the energy when cell i and j are in opposite polarization to each other i.e. if the polarization of cell i is +1 then consider the polarization of cell j as -1 and vice versa. This means, in the $E_{opposite}$ case, the cell j does not follow the desired polarization same as the input cell i polarization. So, $E_{opposite}$ energy can also be considered as the energy for the undesired state of the cell. Likewise, E_{same} is the energy when cell i and j are in the same polarization either +1 or -1. Since both the cells i and j are having the same polarization as desired, this energy is also considered as the

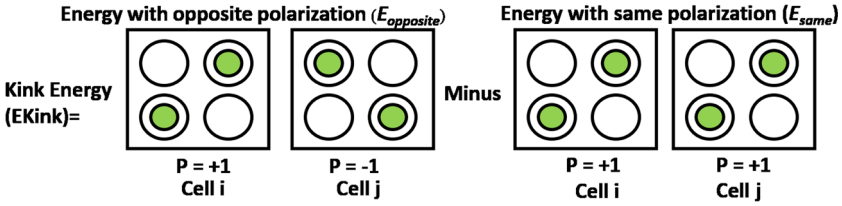

Fig. 6 Interpretation of kink energy

energy for the desired state of the cell. After calculating kink energy, if it comes to be +ve, then nearby cell adopts the same polarization and in case of -ve value, the cell adopts the polarization opposite to its input cell polarization.

Another way to find the position of electrons i.e. the cell polarization is to take the polarization of either $E_{opposite}$ or E_{same} whichever is less. Thus, the output cell polarization of any QCA primitive can be estimated using kink energy.

4.2 Output Cell Polarization Estimation Based on the Kink Energy in Case of Defect Free MV

As, we know that MV is the core element of QCA circuit, we have done the analysis specifically for it. As discussed earlier in above section, the kink energy for defect free MV can be calculated by finding the energies $E_{opposite}$ and E_{same}. Here, the kink energy calculation has been done only for one input combination out of 8 combinations. As output cell of MV always adopts the device (middle) cell polarization, so device cell polarization is considered as the final output polarization of it. Now, $E_{opposite}$ and E_{same} are considered as undesired and desired state of the device cell respectively. $E_{opposite}$ and E_{same} energies are described below in their respective cases:

Case 1: $E_{opposite}$ is the energy when the device cell is in the undesired state. Case 1 is depicted in Fig. 7a. As shown, input A = 0, B = 0 and C = 1. So, as per the functionality of MV, the device cell polarization must be majority of the three inputs i. e. P = -1 or logic 0. Therefore, undesired device cell polarization i.e. P = +1 or logic 1 is considered to calculate $E_{opposite}$ energy in case 1.

Case 2: E_{same} is the energy when the device cell is in the desired state. Case 2 is depicted in Fig. 7b. As shown, device cell polarization is in desired state i.e. P = -1 or logic 0 since input A = 0, B = 0 and C = 1. Therefore, desired device cell polarization is considered to calculate E_{same} energy in case 2.

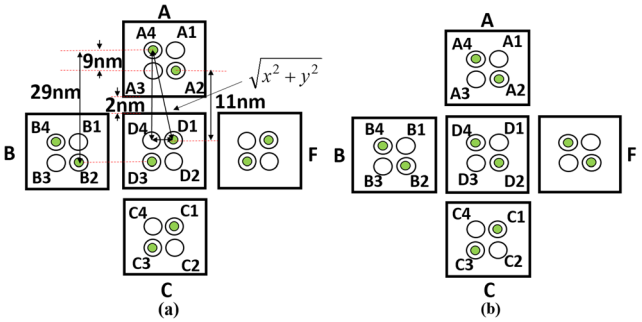

Fig. 7 MV with input combination A = 0, B = 0 and C = 1 and device cell in **a** undesired state for energy $E_{opposite}$ calculation **b** desired sate for energy E_{same} calculation

As per Eq. 9, the electrostatic energy between two cells is inversely proportional to the distance between the two dots in which the electrons are localized. So, to calculate the energies $E_{opposite}$ and E_{same} various distances for MV are to be decided. For this purpose, initially, we have taken value of the cell parameters shown in Fig. 3a as cell height = 18nm, cell width = 18nm, the distance between dots = 9nm, the distance between cells 2nm and dot diameter 5nm. From these cell parameters, the various distances for MV are calculated and shown in Fig. 7a. The device cell's dot numbers are assigned in a clockwise direction from D1 to D4. The diagonal dots in which the electrons are localized for input cell A are labeled as A2 & A4 for P = -1 and A1 & A3 for P = +1. In the same manner, the nomenclature of the diagonal dots in which the electrons are localized for input cells B and C are considered. The distance calculations vary as per the input combinations, since electrons in input cells reside either diagonally right or left according to its polarization or logic value. Hence, dimensions mentioned in Fig. 7a and b would be different depending on the input combination which is taken into consideration while calculating distances and energies for every input combination. Now from these distances the $E_{opposite}$ and E_{same} energies are calculated for both the cases.

Case 1: From the dimensions shown in Fig. 7a, Energy $E_{opposite}$ is calculated in this section for the input combination A = 0, B = 0 and C = 1. The polarization of input cell A is P = -1, it means electrons are localized in A2 and A4 of the input cell A. The polarization of the device cell is considered as P = +1, it means electrons are localized in dot D1 and D3 of the device cell. A4D1 is the distance between dot A4 of the input cell A and dot D1 of the device cell. From Fig. 7a, the X and Y axis distances are 9nm and

20nm respectively for distance A4D1. So, using Pythagoras theorem A4D1 is calculated as 21nm. Now as per the Eq. 9, the energy between cell A and device cell which is equal to the inverse of the distance is calculated as 0.0456* C J, where C is the constant and equal to $\frac{q^2}{4\pi\varepsilon_0\varepsilon_r}$. In the same manner, distances between input cells B and C with respect to device cell is calculated. Then, its corresponding electrostatic energies are calculated. Now, the total energy ($E_{opposite}$) for case 1, when inputs A = 0, B = 0 and C = 1 is the summation of all the energies and given by the Eq. 11.

$$E_{opposite} \cong \frac{1}{A4D1}+\frac{1}{A4D3}+\frac{1}{A2D1}+\frac{1}{A2D3} + \frac{1}{B4D1}+\frac{1}{B4D3}+\frac{1}{B2D1}+\frac{1}{B2D3} + \frac{1}{C1D1}+\frac{1}{C1D3}+\frac{1}{C3D1}+\frac{1}{C3D3} \quad (11)$$

From the Eq. 11, we get $E_{opposite}$ = 0.6365 * C J which is the summation of all the energies between the dots where the electrons are located as per the input combination.

Case 2: As similar to Case 1, from the dimensions shown in Fig. 7a, Energy E_{same} is calculated in this section for the input combination A = 0, B = 0 and C = 1 shown in Fig. 7b. The electrons in device cell are located at number 2 and 4 since its polarization P = -1 or logic 0. A4D2 is the distance between the dot A4 of the input cell and dot D2 of the device cell. From the Fig. 7b, the distances for A4D2 are 9nm and 29nm in X and Y directions respectively. So, using Pythagoras theorem A4D2 is calculated as 30.364nm and its corresponding energy, using Eq. 9 is calculated as 0.0329* C J. In the same manner, distance and energy between input cells B and C with respect to device cell are calculated. So, the energy (E_{same}) for the case 2 when A = 0, B = 0 and C = 1 is given by Eq. 12, it contains the distances between dots in which the charges are located.

$$E_{same} \cong \frac{1}{A4D2}+\frac{1}{A4D4}+\frac{1}{A2D2}+\frac{1}{A2D4} + \frac{1}{B4D2}+\frac{1}{B4D4}+\frac{1}{B2D2}+\frac{1}{B2D4} + \frac{1}{C1D2}+\frac{1}{C1D4}+\frac{1}{C3D2}+\frac{1}{C3D4} \quad (12)$$

Hence, from Eq. 12, we get E_{same} = 0.6232* C J.

Thus for input combination A = 0, B = 0 and C = 1 of MV, energy $E_{opposite}$ = 0.6365* C J, E_{same} = 0.6232* C J. From Eq. 10, E_{kink} = $E_{opposite}$ - E_{same} = 0.013* C J (+ve Value). As discussed, if the kink energy is +ve then nearby cell adopts the polarization as energy E_{same} or of the desired state. Therefore, the device cell polarization P = -1 or logic 0 as desired since A = 0, B = 0 and C = 1.

The polarization of device cell is also found by taking polarization of the least value of two calculated energies $E_{opposite}$ and E_{same}. Here energy E_{same} is the least energy, so the device cell adopts desired state polarization.

In this way, the energy calculations have been carried out for all 8 combinations of inputs A, B, and C. The value of energies $E_{opposite}$, E_{same} and E_{kink} for output estimation of defect free MV are shown in Fig. 8.

In Fig. 8 the base line indicates the energy level of E_{kink} = 0. Energies $E_{opposite}$ and E_{same} are ploted on primary axis whereas, E_{kink} is ploted on secondary axis. When the E_{kink} is +ve, it is above the base line, output polarization P = -1 (logic 0). When the E_{kink} is -ve i.e. below the base line, output polarization P = +1 (logic 1). For example, input combination A = 0, B = 1, and C = 1 the E_{kink} value is below the base line i.e. E_{kink} is -ve. So, the output polarization P = +1 i.e. logic 1 which is the majority of inputs as desired. Kink energy calculations for corresponding input

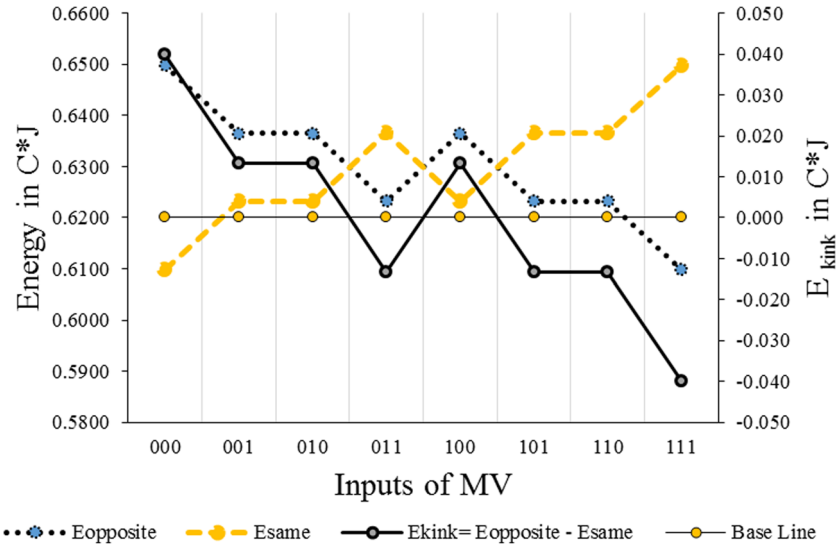

Fig. 8 Energies $E_{opposite}$, E_{same} and E_{kink} values for 8 input combinations of defect free MV

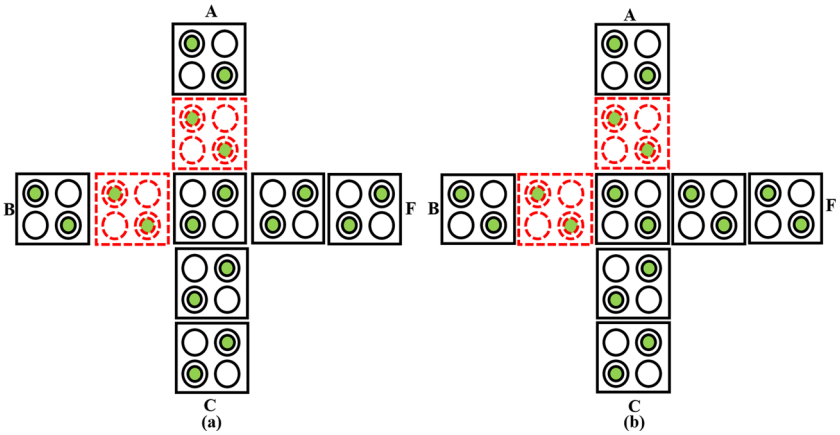

Fig. 9 Representation of MMC defect in MV **a** $E_{opposite}$ energy or undesired state calculations **b** E_{same} energy or desired state calculations

combinations shows that the MV follows the polarization of majority of inputs.

Thus, the developed kink energy based analytical method is useful to estimate the device cell polarization state and the output cell polarization of defect free MV.

4.3 Output Cell Polarization Estimation Based on the Kink Energy in Case of MMC Defect in MV

In this section, the effect of MMC defect is validated using the kink energy based analytical method presented in above section. Consider the multiple missing cells (2,3)&(1,2) of MV shown in Fig. 2a. For kink energy calculations, Fig. 7a and b are referred again as Fig. 9a and b respectively with missing cells (2,3)&(1,2). Input combination of Fig. 9a and b is A = 0, B = 0 and C = 1.

External input cells A, B, and C are assumed to be defect free. The cells (2,3)&(1,2) are removed from the MV configuration as shown in Fig. 9a and b. Accordingly, distances are calculated and its corresponding energies $E_{opposite}$ and E_{same} have been calculated. Subsequently, kink energy E_{kink} is calculated for the input combination A = 0, B = 0 and C = 1, the value of $E_{opposite}$ = 0.40619* C J, E_{same} = 0.41869* C J and E_{kink} = -0.01250* C J. So, the output polarization in case of the missing cell (2,3)&(1,2) for this input combination is P = +1. In this way, the energies are calculated for all 8 input combinations and shown in Fig. 10.

It is observed from the calculated energies as mentioned in Fig. 10 that the output polarization is always same as the input C polarization. Thus the fault for this missing cells from the kink energy calculation is s-a-C, same as obtained by the simulation and mentioned in Table 3.

In this way, $E_{opposite}$, E_{same} and E_{kink} energies are calculated for all MMC defect for MV mentioned in Table 3 and other QCA devices as well. The similar results are obtained from both the simulation based analysis and kink energy based mathematical calculations.

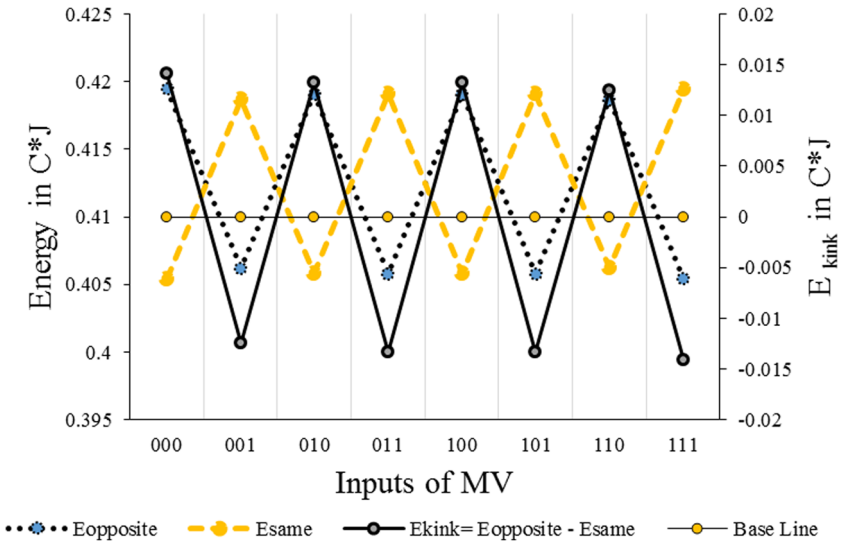

Fig. 10 Energies $E_{opposite}$, E_{same} and E_{kink} values for missing cells (2,3) & (1,2)

Fig. 11 Verilog module for MV including MMC defect modeling

```
module MMC_MV (A, B, C, F ,fault0, fault1, fault2);
     input A,B,C;
     input fault0, fault1, fault2;
     output F;
     wor wi1, wi3;
     wor F;
     // fault0,fault1,fault2 000 op = wi1 //(fault free)
     //010 op = B
     //100 op = wi3 //(Maj(A',B,C'))
     //110 op = A
     //001 op = C
     //011 op = A`
     //101 op = C`
     //111 op = (Low Polarization)
     assign wi1 = (A & B) | (B & C) | (A & C);
     assign wi3 = (~A & B) | (B & ~C) | (~A & ~C);
     assign F = (fault2) ? ((fault0) ? ((fault1) ? 1'bZ: ~C ) :
                ((fault1) ? ~A: C )) :((fault0) ? ((fault1) ? A: wi3 ) :
                ((fault1) ? B: wi1 ));

endmodule
```

5 Proposed HDL Models for MMC Defect

In this section, the HDL model is proposed for MMC defect. Such model helps in verifying the functionality and timing of QCA circuits by fault injection at logic level. The HDL-Verilog is used to implement the fault activation features in all QCA devices at the logic level. Example of MV module is presented in this paper. The snapshot of developed MV module for activation of faults caused by MMC defect is shown in Fig. 11.

As per Table 3, six fault sets namely s-a-A, s-a-A', s-a-B, s-a-C, s-a-C', F(A',B,C') and low polarization caused by MMC defect in MV are identified. To activate this fault set, three auxiliary inputs *fault0, fault1* and *fault2* are added to the MV module. As per the status of these auxiliary inputs, the corresponding fault can be activated as mentioned in Table 8.

Now, consider the s-a-A' fault in MV caused by MMC defect, this is activated when *fault0* = 0, *fault1* = 1 and *fault2* = 1. The simulation result for this fault is shown in Fig. 12.

Similarly, all stuck-at-faults caused by the MMC defect in MV are verified by logic level simulation. The similar HDL model is developed for other QCA primitives like inverter and various wires. Basically, these modules are developed using Verilog with fault activation capabilities. By instantiating required modules, design top module can be developed. Hence, the developed HDL model supports verification of top module functionality along with analysis of faults caused by the MMC defect in all QCA primitives of it. The developed HDL model is useful to analyze the effect on a circuit output at the logic level under the influence of faults caused by MMC defect.

Table 8 Values of *fault0, fault1, fault 2* and its corresponding fault

Auxiliary input			Fault
fault 0	*fault1*	*fault2*	
0	0	0	F(A,B,C)
0	0	1	s-a-C
0	1	0	s-a-B
0	1	1	s-a-A'
1	0	0	F(A',B,C')
1	0	1	s-a-C'
1	1	0	s-a-A
1	1	1	LP

6 Analysis of MMC Defect at the Circuit Level

6.1 MMC Defect When Device is Non-Primary Output of a Circuit

The defect analysis of QCA logical devices i.e. MV and inverter were done in standalone mode i.e. the output is directly observed from the primitive as PO in Section 3. In this section, we are analyzing the same defects in case of these devices are part of a circuit i.e. connected with other primitive, mostly wires. It has been observed that when the output of QCA primitive is connected with wire, in presence of wire, the MMC defect behaves differently and needs to analyze. Mostly, low polarization is observed when the output cell is missing with any other cell. But due to the regenerative effect of the cell to cell response, if the output cell of primitive is no longer a standalone cell then low polarization effect is not propagated. Therefore, the effect of MMC defect on the QCA devices in case of output as non PO for MV is presented in Table 9.

In case of the inverter, cell numbers of the inverter shown in Fig. 2b are considered. If output cell (5,2) is not PO & it is missing with any another cell except cell (2,2) then the functionality of the inverter will not get affected, only when it is missing with the cell (2,2), inverter acts as a binary wire.

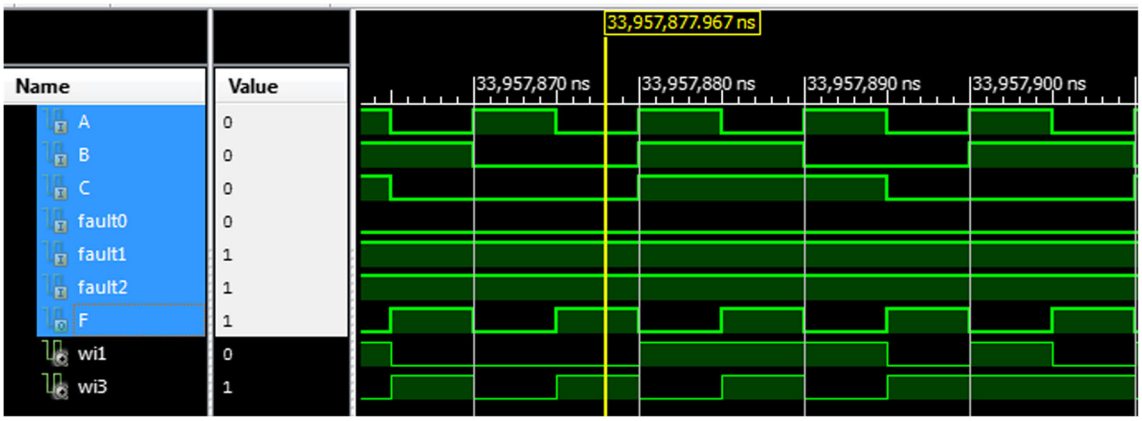

Fig. 12 Simulation result of MV for s-a-A' fault when *fault0* = 0, *fault1* = 1 and *fault2* = 1

Otherwise, in most of the cases when output cell is missing, inverter function properly.

6.2 MMC Defect Analysis of EXOR Gate

The proposed MMC defect at the circuit level i.e. in EXOR gate is analyzed. For this purpose, the layout of EXOR gate is implementation using QCADesigner and shown in Fig. 13.

The MMC defect analysis of EXOR gate in the QCA devices for respective faults are summarized in Table 10. Also, as mentioned in Table 10, the fault in place of low polarization in case of this non PO output are considered for the analysis. Low polarization at the output of EXOR gate

Table 9 Effect of MMC defect on MV when output cell of MV is PO and non PO

Sr. No.	Missing cell numbers	Output of MV if F is PO	Output of MV if F is not PO
1	(2,3)&(1,2)	C	C
2	(2,3)&(2,1)	B	B
3	(2,3)&(2,2)	C'	C'
4	(2,3)&(3,2)	**LP**	**B**
5	(1,2)&(2,1)	A	A
6	(1,2)&(2,2)	F(A'BC')	F(A'BC')
7	(1,2)&(3,2)	**LP**	**F(ABC)**
8	(2,1)&(2,2)	A'	A'
9	(2,1)&(3,2)	**LP**	**B**
10	(2,2)&(3,2)	**LP**	**F(A'BC')**
11	(2,3)&(1,2)&(2,1)	F(ABC)	F(ABC)
12	(2,3)&(1,2)&(2,2)	C'	C'
13	(2,3)&(1,2)&(3,2)	**LP**	**C**
14	(2,3)&(2,1)&(2,2)	B	B
15	(2,3)&(2,2)&(3,2)	**LP**	**C'**
16	(1,2)&(2,1)&(2,2)	A'	A'
17	(1,2)&(2,1)&(3,2)	**LP**	**A**
18	(1,2)&(2,2)&(3,2)	**LP**	**F(A'BC')**
19	(2,1)&(2,2)&(3,2)	**LP**	**A'**
20	(2,3)&(2,1)&(3,2)	**LP**	**B**
21	(2,3)&(1,2)&(2,1)&(2,2)	C'	C'
22	(2,3)&(1,2)&(2,2)&(3,2)	LP	Not valid
23	(2,3)&(2,1)&(2,2)&(3,2)	LP	Not Valid
24	(1,2)&(2,1)&(2,2)&(3,2)	LP	Not Valid
25	(2,3)&(1,2)&(2,1)&(3,2)	LP	Not Valid

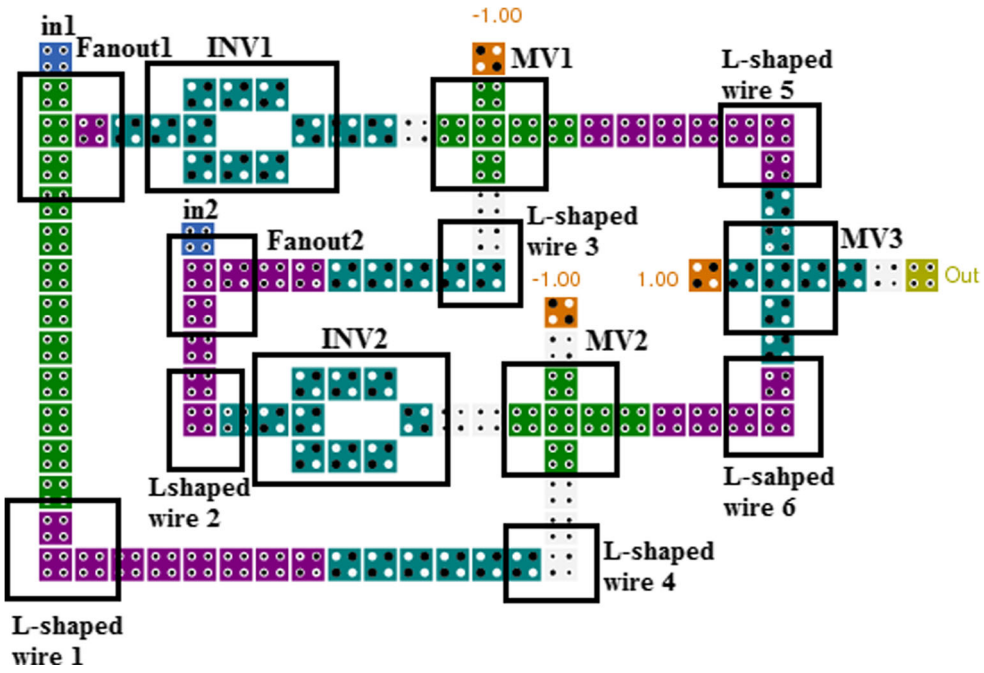

Fig. 13 The layout of QCA EXOR gate using QCA devices

Table 10 Results of MMC defect in EXOR gate

QCA device	Fault	Output of device	Output of EXOR gate	In1 In2	Out Z/Zf
MV1	s-a-B	In1’	In1’+In1In2’	00	0/1
	F(A’BC’)	In1’+In2’	In1’+In2’	00	0/1
	s-a-A	0	In1In2’	01	1/0
	s-a-A’	1	1	00	0/1
				11	0/1
	s-a-C	In2	In2+In1In2’	00	0/1
				11	0/1
	s-a-C’	In2’	In2’+In1In2’	00	0/1
				11	0/1
MV2	s-a-B	In2’	In1’In2+In2’	00	0/1
	F(A’BC’)	In2’+In1’	In1’+ In2’	00	0/1
	s-a-A	0	In1’In2	10	1/0
	s-a-A’	1	1	00	0/1
				11	0/1
	s-a-C	In1	In1’In2+In1	11	0/1
	s-a-C’	In1’	In1’	00	0/1
				10	1/0
MV3	s-a-B	1	1	00	0/1
				11	0/1
	F(A’BC’)	1	1	00	0/1
				11	0/1
	s-a-A	In1’In2	In1’In2	10	1/0
	s-a-A’	In1+In2’	In1+In2’	00	0/1
				01	1/0
				11	0/1
	s-a-C	In1In2’	In1In2’	01	1/0

Table 10 (continued)

QCA device	Fault	Output of device	Output of EXOR gate	In1 In2	Out Z/Zf
	s-a-C'	In1'+In2	In1'+In2	00	0/1
				01	1/0
				10	1/0
	LP	LP	LP	Undetect	
INV1	s-a-A	In1	In1.In2+In1In2'	01	1/0
				11	0/1
INV2	s-a-A	In2	In1'In2+In1In2	10	1/0
				11	0/1
Fanout	s-a-A'	In1'	In1In2+In1In2'	01	1/0
Wire 1				11	0/1
Fanout	s-a-A'	In2'	In1'In2'+In1In2'	00	0/1
Wire 2				01	1/0
L-shaped	s-a-A'	In1'	In1'In2'+In1In2'	00	0/1
Wire 1				01	1/0
L-shaped	s-a-A'	In2'	In1'In2+In1In2	10	1/0
Wire 2				11	0/1
L-shaped	s-a-A'	In2'	In1'In2'+In1In2'	00	0/1
Wire 3				01	1/0
L-shaped	s-a-A'	In1'	In1'In2+In1'In2'	00	0/1
Wire 4				10	1/0
				11	0/1
L-shaped	s-a-A'	(In1'In2)'	(In1'In2)'+In1In2'	00	0/1
Wire 5				01	1/0
				11	0/1
L-shaped	s-a-A'	(In1In2')'	In1'In2+(In1In2')'	00	0/1
Wire 6				10	1/0
				11	0/1

is observed when output cell of MV3 is missing with any other cell or cells since it is PO of the EXOR gate. Hence, This fault is undetectable. The possible test vector to detect the fault caused by the MMC defect and its corresponding fault free and faulty value are mentioned in Table 10. As the output of MV1 and MV2 is not PO of the EXOR gate, low polarization effect is not observed in both of the MVs.

In this way, the fault effects caused by the MMC defect in QCA devices are analyzed at the circuit level. It is observed that the device level effects are propagated to the circuit level. Hence, the device level fault sets caused by the MMC defect in respective devices have been validated at the circuit level.

Also, the effects on the output of EXOR gate at the logic level are analyzed using developed HDL model for MMC defect. For this purpose, required modules are instantiated. The obtained results at the logic level are similar to the results obtained at the layout level for the EXOR gate.

7 Comparison Between Test Vector Sets of SMC and MMC Defects

Test vector set to detect the stuck-at-faults caused by single missing and multiple missing cells defects for MV, MV_AND and MV_OR are identified. These are mentioned in Table 11. Input is ABC, fault free and faulty output is Z and Zf.

Following conclusion is drawn from the Table 11:

1. In case of MMC defect, complete test set S for MV is the union of complete test sets S0 and S1 where the S0 and S1 are the complete test set for MV_AND and MV_OR respectively.
   $\{S\} = \{S0 \bigcup S1\}$
2. In case of MMC defect, the intersection of complete test sets S0 and S1 is NULL set where the S0 and S1 are the complete test set for MV_AND and MV_OR respectively.
   $\{S0 \bigcap S1\} = \{\phi\}$

Table 11 Test vector sets for MV, MV_AND and MV_OR

Possible	MV_AND		MV_OR		MV	
Faults	ABC	Z/Zf	ABC	Z/Zf	ABC	Z/Zf
s-a-B	010	0/1	101	1/0	010	0/1
					101	1/0
s-a-A	100	0/1	011	1/0	011	1/0
					100	0/1
s-a-A'	000	0/1	001	0/1	000	0/1
					001	0/1
	010	0/1	101	1/0	010	0/1
					101	1/0
	110	1/0	111	1/0	110	1/0
					111	1/0
s-a-C	110	1/0	001	0/1	001	0/1
					110	1/0
s-a-C'	000	0/1	011	1/0	000	0/1
					010	0/1
	010	0/1	101	1/0	011	1/0
					100	0/1
	100	0/1	111	1/0	101	1/0
					111	1/0
F(A'BC')	000	0/1	101	1/0	000	0/1
					010	0/1
	010	0/1	111	1/0	101	1/0
					111	1/0

8 Conclusion

In this paper, the importance of Multiple Missing Cell (MMC) for QCA devices has been shown in length. The proposed MMC defect modeling is backed by exhaustive simulation and mathematical analysis. The Verilog model of QCA primitives for MMC defect is proposed which can be further used in functional and timing verification, and activation of faults caused by MMC defect in QCA circuit. Also, testing properties are proposed which can be used for test devlopment process. The future work is to develop the effective test pattern generation algorithm for the proposed MMC defect.

Acknowledgements We are thankful to Dr. K. S. Dasgupta, Director, DAIICT, Gandhinagar, India, Dr. Manoj Singh Gaur, Director, IIT, Jammu, India and Dr. Virendra Singh, Associate Professor, IIT, Bombay, India for their valuable guidance.

References

1. Amlani I, Orlov AO, Kummamuru RK, Bernstein GH, Lent CS, Snider GL (2000) Experimental demonstration of a leadless quantum-dot cellular automata cell. Appl Phys Lett 77(5):738–740
2. Chen K, Maezawa K, Yamamoto M (1996) Inp-based high-performance monostable-bistable transition logic elements (MOBILE's) using integrated multiple input resonant-tunneling devices. IEEE Electron Dev Lett 17(3):127–129
3. Dhare V, Mehta U (2015) Defect characterization and testing of QCA devices and circuits: a survey. In: Proc of 19th international symposium on VLSI design and test, pp 1–2
4. Dhare V, Mehta U (2015) Fault analysis of QCA combinational circuit at layout & logic level. In: Proc of IEEE International WIE conference on electrical and computer engineering, WIECON, pp 22–26
5. Dhare V, Mehta U (2016) Development of basic fault model and corresponding ATPG for single input missing cell deposition defects in majority voter of QCA. In: Proc of IEEE region 10 conference, TENCON, pp 2354–2359
6. Dysart TJ, Kogge PM, Lent CS, Liu M (2005) An analysis of missing cell defects in quantum-dot cellular automata. In: Proc. of IEEE international workshop on design and test of defect-tolerant nanoscale architectures, NANOARCH pp 1–8
7. Huang M, Momenzadeh FL (2007) Analysis of missing and additional cell defects in sequential quantum-dot cellular automata. Integr VLSI J 40(1):503–515
8. Jing Huang M, Momenzadeh MB, Tahoori F (2004) Lombardi: defect characterization for scaling of QCA devices. In: Proc of 19th IEEE international symposium on defect and fault tolerance in VLSI systems, pp 30–38
9. Lent CS, Snider GL (2014) The development of quantum-dot cellular automata. Field coupled nanocomputing, LNCS. Springer, pp 3–20
10. Lent CS, Taugaw PD (1993) Lines of interacting quantum-dot cells: a binary wire. J Appl Phys 74:6227–6233
11. Lent CS, Tougaw PD (1997) A device architecture for computing with quantum dots. Proc IEEE 84(4):541–557
12. Lent CS, Tougaw PD, Porod W, Bernstein GH (1993) Quantum cellular automata. Nanotechnology 4(1):49–57
13. Lent CS, Taugaw PD, Porod W (1994) Quantum cellular automata: the physics of computing with arrays of quantum dot molecules. In: Proc of workshop on physics and computing, pp 5–13
14. Likharev K (1999) Single electron devices and their applications. Proc IEEE 87(4):606–632
15. Liu M, Lent C (2007) Reliability and defect tolerance in metallic quantum-dot cellular automata. J Electron Test 23(3):211–218
16. Meindl J (2003) Beyond Moore's law: the interconnect era. Comput Sci Eng 5(1):20–24
17. Momenzadeh M, Ottavi M, Lombardi F (2005) Modeling qca defects at molecular-level in combinational circuits. In: Proc of 20th IEEE design for test, DFT, pp 208–216
18. Orlov AO, Amlani I, Bernstein GH, Lent CS, Snider GL (1997) Realization of a functional cell for quantum-dot cellular automata. Sci Mag 227:928–930
19. Peercy P (2000) The drive to miniaturization. Nature 406(6799):1023–1026
20. Porod W, Lent CS, Bernstein GH, Orlov AO, Amlani I, Snider GL, Merz JL (1999) Quantum-dot cellular automata: computing with coupled quantum dots. Int J Electron 86(5):549–590
21. Schulhof G, Jullien WK (2007) Simulation of random cell displacement in QCA. ACM J Emerg Technol Comput Syst (JETC) 3(1):1–14
22. Tahoori M, Momenzadeh M, Huang J, Lombardi F (2004) Testing of quantum cellular automata. IEEE Trans Nanotechnol 3(4):432–442
23. Tahoori MB, Momenzadeh M, Huang J, Lombardi F (2004) Defects and faults in quantum cellular automata at nano scale. In: Proc of 22nd IEEE VLSI test symposium, VTS, pp 291–296

24. Toth G, Lent CS (1999) Quasiadiabatic switching for metal-island quantum-dot cellular automata. Appl Phys Lett 85(5):2977–2984
25. Tougaw P, Douglas CS (1994) Lent: logical devices implemented using quantum cellular automata. J Appl Phys 75(3):1818–1825
26. Walus K, Dysart TJ, Jullien GA, Budiman RA (2004) Qcadesigner: a rapid design and simulation tool for quantum-dot cellular automata. IEEE Trans Nanotechnol 3(1):26–31
27. Yang XK, Cai L, Wang SZ, Wang Z, Feng C (2012) Reliability and performance evaluation of QCA devices with rotation cell defect. IEEE Trans Nanotechnol 11(5):1009–1018
28. Zhang Y, Lv H, Liu S, Xiang Y, Xie G (2015) Defect-tolerance analysis of fundamental quantum-dot cellular automata devices. Article in The Journal of Engineering, 1–6

Vaishali H. Dhare has received Diploma in Electrical from Board of Technical Education, Bombay, Maharashtra, B.E. Degree in Electronics and Telecommunication from NMU, Maharashtra and M.Tech degree in Electronics and Communication Engineering (VLSI Design) from the Institute of Technology, Nirma University and Ph.D. degree from Nirma University. Vaishali Dhare is Assistant Professor with the Department of Electronics & Communication Engineering, Institute of Technology, Nirma University, Ahmedabad, India. She is a member of IEEE, ISTE and VLSI Society of India. Her area of interest includes VLSI Design, Testing of VLSI Design, VLSI Physical Design and Hardware Description Languages.

Usha S. Mehta has done her Ph. D. in the area "Testing of VLSI Design" and is currently working as Professor at Nirma University, Ahmedabad. She has more than 22 years of academic experience which includes industrial experience of five years also. She has one patent on her credit. She has published one book and more than 50 research papers in international journals and conferences. She is the reviewer of VLSI related books from reputed publishers like Tata - McGraw-Hill and also involved in reviewing research articles from reputed journals from IEEE, Elsevier and Science-Direct. Her research activity includes the research projects from various organizations like ISRO and GUJCOST. She has successfully organized International Conferences, Symposiums, Seminars, workshops and Training programs for Industry, academia and students. The VDAT-2015 and NUiCONE-2012 are the most successful events coordinated by her as Conference Chairs. She is also Associate Editor, IET - Computers and Digital Techniques Chair, Women-In-Engineering Affinity Group, IEEE Gujarat Section and Senior Member, IEEE.